Research Article

José Carrión*, Fredy Flores, Freddy Rodríguez, and Miguel Pozo

Global Geopotential Models assessment in Ecuador based on geoid heights and geopotential values

https://doi.org/10.1515/jogs-2022-0165 received June 12, 2023; accepted December 8, 2023

Abstract: Since the 1960s, the analysis of disturbed satellite orbits to infer Earth's gravity field functionals has been an important element in determining the Earth's gravitational field. The long wavelengths of the gravitational field are recovered through the analysis of non-Keplerian variations in the orbital path of artificial satellites, from their tracking from ground stations (Satellite Laser Ranging, Doppler Orbitography and Radiopositioning Integrated by Satellite, and Precise Range And Range-Rate Equipment), from satellite-to-satellite tracking, or by microwave interferometry. In addition, differences in gravitational acceleration in three mutually orthogonal dimensions can be determined by employing a differential accelerometer carried on artificial satellites (satellite gravity gradiometry, SGG). Satellite gravimetry provides global information (long wavelengths) of the Earth's gravitational field, which is the fundamental basis for the implementation of Global Geopotential Models (GGMs). The GGMs are one of the key tools for the representation of the Earth's gravity field and, therefore, for the establishment of a Global Height System (i.e., International Height Reference System), whose fundamental reference surface is defined in terms of a geopotential value. In this study, the validation of high-resolution GGMs (coefficients up to degree 2190) was performed based on their performance in Ecuador by comparing geoid heights estimated by the GGMs with the corresponding values derived from Global Navigation Satellite System/leveling records. Furthermore, geopotential values from the GGMs are compared with the corresponding value obtained for the Ecuadorian Vertical Datum by solving the fixed geodetic boundary value problem. The obtained results indicated that the precision of the high-resolution GGMs does

not reach the established requirements for the geopotential computation in the International Height Reference Frame fundamental stations.

Keywords: Global Geopotential Model, Global Height System, geoid heights, International Height Reference System, International Height Reference Frame.

1 Introduction

The Global Geopotential Models (GGMs), according to Pavlis (2013), are mathematical approximations of the external gravitational potential of an attractive body (the Earth in the case of geodesy). A GGM consists of a set of numerical values for certain parameters, statistics of errors associated with these values, and a collection of mathematical expressions, numerical values, and algorithms that allow calculating magnitudes related to gravitational potential (synthesis) and associated errors (error propagation based on a covariance matrix). The development of a high-resolution GGM involves the appropriate combination of varied information from orbital platforms, ground surveys, ocean surveys, airborne sensors, and altimetry. Combined models associate various sources of gravity information (satellite orbits, satellite gravimetry missions, terrestrial, aerial and oceanic gravimetry, satellite altimetry, and Digital Elevation Models) with reduced omission errors (or truncation), but with great dependence on commission errors due to the diversity of references involved.

GGMs have both operational and scientific uses. Among the most important, we can mention the following: determination of satellite orbits; determination of the trajectory of missiles and aircraft (inertial navigation); calculation of geoid heights; the estimate of the Dynamic Ocean Topography, or even of the Mean Ocean Dynamic Topography; study of the ocean circulation for marine applications; realization of the Global Vertical Datum (GVD), considering as a reference the geopotential surface materialized by a GGM; and geophysical prospecting (determination of mass distribution) (Pavlis, 2013).

Fredy Flores, Freddy Rodríguez, Miguel Pozo: Department of Geodesy – Geographic Military Institute of Ecuador, Quito, Ecuador

^{*} Corresponding author: José Carrión, Department of Geodesy – Geographic Military Institute of Ecuador, Quito, Ecuador, e-mail: josecarrionsa@gmail.com

Among the applications of the GGMs and emphasizing the establishment of the geodetic reference frame, we highlight in this manuscript the realization of the GVD as an equipotential surface of the Earth's gravity field with geopotential W_0 . The GVD represents one of the key elements for the establishment of a Global Height System, as indicated by the International Association of Geodesy (IAG) in its resolution for the definition and realization of the International Height Reference System (IHRS) (Drewes et al., 2016).

According to the conventions established by the IAG (Drewes et al., 2016) and disseminated at the regional level by Geodetic Reference System for the Americas (SIRGAS), in relation to the establishment of a Global Vertical Reference System, the heights belonging to the fundamental leveling networks must be obtained according to the calculation of geopotential numbers (C) and be linked to a GVD (materialized by an equipotential surface of the Earth's gravity field with a geopotential value $W_0 = 62636853.4$ m² s⁻²) (Ihde et al., 2017).

Furthermore, as stated by Ihde et al. (2017), the IHRS realization (International Height Reference Frame [IHRF]) requires the combination of a global station network, a GGM, and a set of parameters. Thus, the long and medium wavelengths of the gravity field, recovered from a GGM, are one of the key elements for determining geopotential values for the fundamental stations constituting the IHRF.

The evolution towards a GVD has originated in several countries with the beginning of activities aimed at the realization of reference stations linked to the GVD (IHRF stations), considering mainly the calculation of the discrepancy $\delta W = W_0 - W_0^i$. In the SIRGAS region, the countries' members have started activities aimed at the realization of a Global Vertical Reference System for the determination of physical heights and referred to GVD. These activities are currently focused on the determination of the optimal positions (according to Ihde et al. (2017), "the stations must be at least continuously monitored to detect deformations, referred to the International Terrestrial Reference System/International Terrestrial Reference Frame (ITRF), and be connected by levelling with the local vertical datum") and the geopotential calculation for the IHRF stations, which serve as fundamental geodetic marks for the IHRS realization (Blitzkow et al., 2017; Carrión et al., 2023; Carrión Sánchez et al., 2018; Guimarães et al., 2021, 2022; SIRGAS WG-III, 2021; Tocho and Vergos, 2016; Tocho et al., 2022, 2023).

As mentioned by Sánchez et al. (2021), a pragmatic way for the calculation of geopotential numbers referred to an equipotential surface of the gravity field is the direct calculation of W(P), which is accomplished by introducing the ITRF coordinates (Altamimi et al., 2016) of a point into the harmonic expansion corresponding to a high-resolution

GGM. In this sense, it should be highlighted the technological advances in satellite gravimetry achieved with the Gravity Recovery and Climate Experiment (GRACE) (Tapley et al., 2004) and Gravity Field and Steady-State Ocean Circulation Explorer (GOCE) missions (Drinkwater et al., 2003), reaching accuracies of $\pm 0.2\,\mathrm{m}^2\,\mathrm{s}^{-2}$ (equivalent to a vertical positional accuracy of $\pm 2\,\mathrm{cm}$) for medium and long wavelengths of the gravity signal, i.e., to a maximum spatial resolution of 100 km (Rummel et al., 2002).

Furthermore, geopotential values W_P can also be calculated by solving the geodetic boundary value problem (GBVP) for regional pure gravimetric geoid/quasigeoid determination, considering the remove-compute-restore scheme. In this case, the information derived from the GGMs is also fundamental. Thus, one of the main inputs for the calculation of geopotential values in IHRF stations is the knowledge of the long (up to degree 70), medium (up to degree 200), and short (about degree 250–200) wavelengths of the gravity field (Sánchez et al., 2021), which can be obtained from the high-resolution GGM. In this sense, it is evident that there is a need to carry out studies that allow its validation in local and regional scenarios. In the present work, geoid heights from GGMs are compared with geoid heights obtained for the level references of the Ecuadorian vertical control network.

Several studies have been carried out with the purpose of validating the GGMs. These works are based on comparing quantities such as geoid heights, gravity anomalies, and gravity disturbances with those derived from global models. The Ecuadorian Vertical Reference System (EVRS) must adapt to the precepts established by the IAG and disseminated in South America by SIRGAS. The establishment of the vertical datum for the EVRS must be based on the calculation of the geopotential (W_0^i) at one or more fundamental stations (i.e., IHRF stations).

2 Methods

The GGMs are implemented based on a spherical harmonic expansion; the low and medium frequencies of the series are derived from the analysis of the satellite orbits, the satellite-to-satellite tracking, and gravimetric gradiometry. The high degree and order of expansion are achieved by combining the information from satellites with terrestrial-oceanic gravimetry, Digital Elevation Models, and products derived from satellite altimetry (Torge and Müller, 2012).

Geodesists have used several methods to represent the Earth's gravity field, and among these methods are mass points (Sünkel, 1981), finite elements (Meissl, 1981), and splines (Sünkel, 1984). Earth's gravity field modelling using

these approaches is limited to some specific applications, while the representation with spherical harmonics has prevailed as the standard method for representing the gravity field globally. The external gravitational potential (V) of a point P defined by its geocentric distance (r_p) , geocentric colatitude (θ_P), and longitude (λ_P) can be calculated according to the following expression (Heiskanen and Moritz, 1985):

$$V(r_P, \theta_P, \lambda_P) = \frac{GM}{r_P} \left[1 + \sum_{n=2}^{\infty} \left(\frac{a}{r_P} \right)^n \sum_{m=-n}^n C_{nm} S_{nm}(\theta_P, \lambda_P) \right]. \quad (1)$$

It is observed that in equation (1), the coefficients of degree and order one (C_{10} , C_{11} , and S_{11}) were assumed to be equal to zero (it refers to the first-order moments of inertia that determine the coordinates of the center of mass), which implies assuming that the system originates from the center of mass. Being GM the geocentric gravitational constant. GM is a constant, and a related to the spheroidal model, that acts as a scale factor associated with the fully normalized spherical harmonic coefficients (C_{nm}). The surface harmonic functions S_{nm} are defined as follows:

$$S_{nm}(\theta_P, \lambda_P) = \bar{P}_{n|m|}(\cos \theta_P). \begin{cases} \cos m\lambda_P \\ \cos |m|\lambda_P \end{cases} \quad \text{para} \quad m \ge 0,$$
 (2)

where $\bar{P}_{n|m|}(\cos\theta_P)$ is the fully normalized Legendre function with degree n and order m.

Gravity field modelling allows the estimation (in the most accurate way) of the C_{nm} coefficients through the optimal combination of gravity information from various data sources. The C_{nm} coefficients are used for the calculation of various functionals of the Earth's gravity field, and therefore, the estimation of the errors associated with these coefficients is an important aspect of model generation (Pavlis, 2013).

The zero-degree term, on the geopotential quantities calculation, refers to the difference (W_0-U_0) between the geopotential W_0 adopted as vertical datum (e.g., which was selected as datum for the IHRF; Drewes et al., 2016) and the normal potential U_0 corresponding to a specific reference ellipsoid. Furthermore, the zero-degree term also takes into account the difference between the GGM's geocentric gravitational constant (GM_{GGM}) and the corresponding geocentric gravitational constant associated with the reference ellipsoid (GM_{GRS}) (e.g., GRS80) (Lemoine et al., 1997).

Thus, the zero-degree term, referring to the calculation of the anomalous potential (T_0) , is given as follows (Hofmann-Wellenhof and Moritz, 2006):

$$T_0 = \frac{GM_{GGM} - GM_{GRS}}{r} - (W_0 - U_0).$$
 (3)

In the present study, the validation of the GGMs shown in Table 1 is accomplished in terms of geoid heights, using

Table 1: GGMs and main characteristics

GGM	n _{max}	Data source
EIGEN-6C4 (Förste et al., 2014)	2,190	A, G, S (GOCE, GRACE, laser geodynamics satellite)
EGM2008 (Pavlis et al., 2008)	2,190	A, G, S (GRACE)
GECO (Gilardoni et al., 2016)	2,190	EGM2008, S (GOCE)
SGG-UGM-1 (Liang and Reißland, 2018)	2,159	EGM2008, S (GOCE)
SGG-UGM-2 (Liang	2,190	A, EGM2008, S (GOCE,
et al., 2020)		GRACE)
XGM2019e (Zingerle et al., 2020)	2,190	A, G, S (GOCO06s), T

In the data source description, A means altimetry, S: satellite, G: ground data, and T: topography.

Global Navigation Satellite System (GNSS)/lev records collected within Ecuadorian territory (Figure 1) and also considering geopotential values for the Ecuadorian Vertical Datum (EVD).

In addition to the analysis carried out with the GNSS/ lev records, geopotential values derived from GGM's height anomalies were evaluated through comparison with the

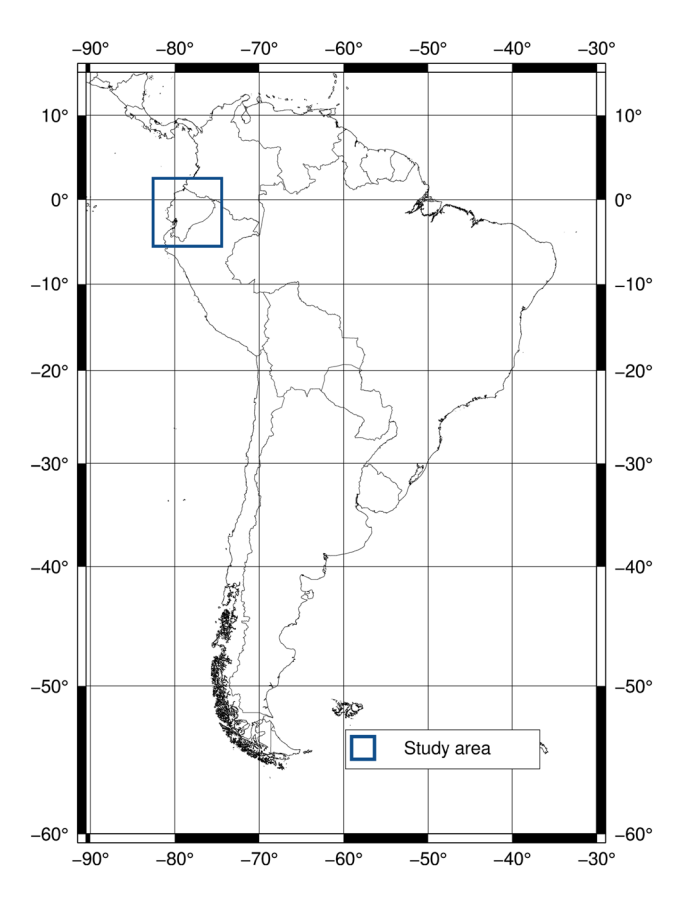


Figure 1: Study area.

geopotential value obtained for the EVD as a solution to the fixed GBVP (Carrión et al., 2023).

The analyses were carried out with the following combined GGMs: EIGEN6C4 (Förste et al., 2014), EGM2008 (Pavlis et al., 2012), GECO (Gilardoni et al., 2016), SGG-UGM1 (Liang and Reißland, 2018), SGG-UGM2 (Liang et al., 2020), and XGM2019e (Zingerle et al., 2020).

2.1 GNSS/lev records

Geometric leveling does not consider the effect of the non-parallelism among the equipotential surfaces of the gravity field. The determination of orthometric heights (*H*) requires the availability of gravity records along the spirit levelling lines. Since not all leveling records from Ecuador's vertical control network have associated gravity observations (gravity observations have been carried out on 3,236 level references from 4,192 – Figure 2), gravity values for the remaining records were obtained through interpolation from existing gravity data.

To predict gravity values, the least-squares collocation method, which is implemented in the PREDGRAV computational package, was used (Drewes, 1976, 1978). Thus, gravity within a radius of 100 km or the nearest 50 records from the interpolated points was considered. PREDGRAV performs interpolation for simple Bouguer anomalies (Δg_B) (4) and

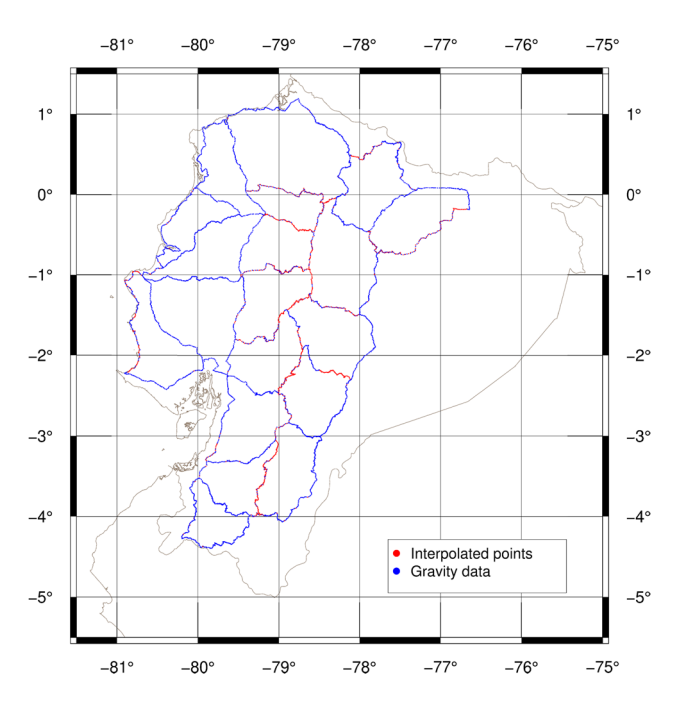


Figure 2: Observed and predicted gravity data for the Ecuadorian vertical control network.

then, following the inverse procedure, calculates the interpolated gravity values.

$$\Delta g_R = g + C_{FA} + C_B - \gamma, \tag{4}$$

where g is the observed gravity, C_{FA} is the free-air correction, C_B is the Bouguer correction, and γ is the normal gravity.

To evaluate the predicted values, we followed a cross-validation procedure, considering 323 gravity records that were randomly selected to cover 10% of the entire gravity dataset. The corresponding statistical values are presented in Table 2.

Thus, the orthometric correction was applied according to the expression given by Heiskanen and Moritz (1967):

$$OC_{AB} = \int_{A}^{B} \frac{g - \gamma_0}{\gamma_0} \Delta n + \frac{g_A - \gamma_0}{\gamma_0} H_A - \frac{g_B - \gamma_0}{\gamma_0} H_B, \quad (5)$$

where OC_{AB} is the orthometric correction for the segment defined between points A and B, Δn is the levelling increment, g is the average gravity along the levelling line, γ_0 is the normal gravity for a standard latitude, and g_A and g_B are the mean gravity values along the plumb line between the physical surface and the geoid.

For the calculation of g_A and g_B , the simplified prey reduction was used considering a normal density of $\rho = 2.67 \, \mathrm{g \, cm^{-3}}$.

$$g = g + 0.0424H. (6)$$

 H_A and H_B are the corresponding orthometric heights for the leveling segment and are calculated iteratively as follows:

$$H_{\text{ort}} = H_{\text{lev}} + \text{OC}.$$
 (7)

Then, orthometric ($H_{\rm ort}$) and ellipsoidal heights (h) for Ecuadorian vertical control network records are used to infer geoid heights such as this expression:

$$N \approx h - H_{\rm ort}. \tag{8}$$

Geoid heights obtained from equation (8) are used to validate geoid heights (*N*) obtained from GGMs. For this study, 3,104 GNSS/lev records from the Ecuadorian vertical control network were used (Figure 3). All the calculations

Table 2: Statistical for predicted gravity from the cross-validation procedure (values in mGal)

Min.	-28.30
Max.	13.34
Mean	-0.10
Std.	2.69

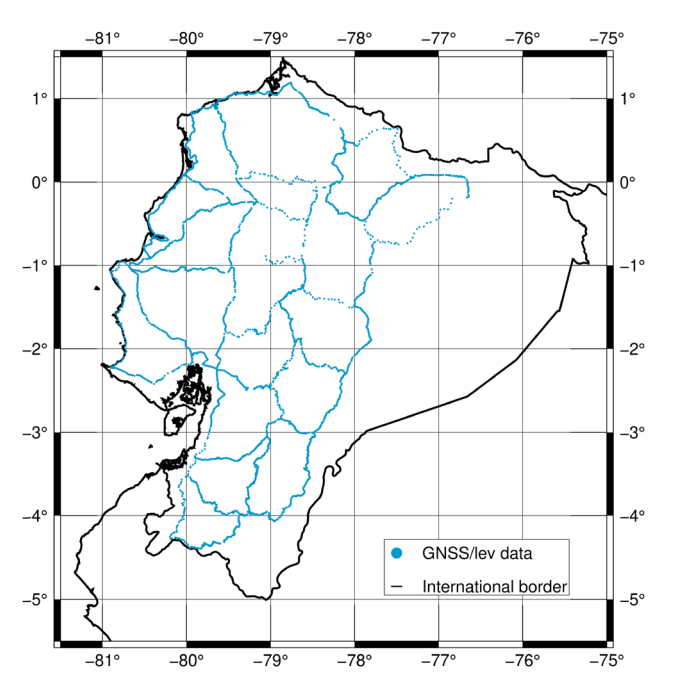


Figure 3: GNNS/lev data.

were performed considering the mean-tide concept, thus the ellipsoidal heights from Global Navigation Satellite System (GNSS) positioning are transformed from the tidefree to the mean-tide concept, according to the expression given by Rapp (1989):

$$H_{\text{mean-tide}} = H_{\text{tide-free}} - (1 + k - h) \frac{\Delta W_{\text{zero-tide}}}{g}, \quad (9)$$

where h and k are the *love* numbers (h = 0.605; k = 0.30190), and the term $\frac{\Delta W_{zero-tide}}{\sigma}$ is obtained with sub-centimeter accuracy as follows (Heikkinen, 1978):

$$\frac{\Delta W_{\rm zero-tide}}{g} \approx -0.198 \left(\frac{3}{2} \sin^2 \bar{\varphi} - \frac{1}{2} \right) [m], \tag{10}$$

where $\bar{\varphi}$ is the geocentric latitude of the calculation point.

2.2 Geoid heights from GGMs

The geoid heights from the GGMs are obtained from the International Center for Global Gravity Field Models (ICGEM) (Ince et al., 2019), considering, for all cases, its maximum degree, the zero-tide as a permanent tide system. The calculation of the geoid heights (N) from a GGM is given as follows (Barthelmes, 2013):

$$N_{\text{GGM}} = \frac{\text{GM}}{r_e \gamma(r_e, \varphi)} \sum_{\ell=0}^{\ell} \sum_{\ell=0}^{\max} \left(\frac{R}{r_e} \right)^{\ell} \sum_{m=0}^{\ell} P_{\ell m}(\sin \varphi) (C_{\ell m}^T \cos m\lambda)$$

$$+ S_{\ell m}^T \sin m\lambda) - \frac{2\pi G\rho}{\gamma(r_e, \varphi)}$$

$$\times \left[R \sum_{\ell=0}^{\ell} \sum_{m=0}^{\max} P_{\ell m}(\sin \varphi) (C_{\ell m}^{\text{topo}} \cos m\lambda + S_{\ell m}^{\text{topo}} \sin m\lambda) \right]^2,$$
(11)

where ℓ and m are the degree and order of spherical harmonic, $P_{\ell m}$ are the fully normalized Legendre functions; GM is the geocentric gravitational constant; $C_{\ell m}^T$ and $S_{\ell m}^T$ are the coefficients of the expansion, usually scaled by the reference radius R; and r_e (latitude dependent), λ , and φ are the spherical geocentric coordinates of the computation point. The second term in equation (11) corresponds to the geoid/quasi-geoid separation (geoid height-height anomaly difference), considering for this a topography model expressed as a surface spherical harmonics expansion, with coefficients $C_{\ell m}^{\text{topo}}$ and $S_{\ell m}^{\text{topo}}$ (Barthelmes, 2013).

Finally, equivalent to the calculation of the zero-degree term for the anomalous potential (equation (3)), the zerodegree term for geoid heights (N_0) is calculated as follows (Rapp, 1997):

$$N_0 = \frac{GM_{GGM} - GM_{GRS}}{r_{P_0}. \gamma_{Q_0}} - \frac{(W_0 - U_0)}{\gamma_{Q_0}},$$
 (12)

where r_{P0} and γ_{O_0} are correspondingly the geocentric radial distance and the normal gravity on the geoid. Moreover, to be consistent with the tide concept used for the values derived from the GNSS/lev records ($N_{\rm GNSS/lev}$), the geoid heights from GGMs are also expressed in the mean-tide concept. For this purpose, the geoid heights computed with equation (8) were transformed to the mean-tide concept, according to the following expressions (Ekman, 1989):

$$N_{\text{mean-tide}} = N_{\text{tide-free}} + (1 + k)(9.9$$

- 29.6 sin² φ)10⁻², $N_{\text{mean-tide}}$ (13)
= $N_{\text{zero-tide}} + (9.9 - 29.6 \sin^2 \varphi)$ 10⁻².

2.3 Geoid height discrepancies and outlier detection

The calculation of discrepancies (ΔN , equation (14)) between geoid heights for the level references (N) and those from the GGMs (N_{GGM}) was carried out initially for an outlier detection's stage, considering only the geoid heights

Table 3: Outlier elimination N_r statistics

	Before outlier exclusion	After outlier exclusion
Min. (m)	-3.620	-0.967
Max. (m)	3.531	1.071
Mean (m)	0.047	0.018
Std. (m)	0.509	0.379
N°	3104	3000
%	100	96.65

coming from the GGM XGM2019e at its maximum degree (Förste et al., 2014).

$$\Delta N = N_{\text{GNSS/lev}} - N_{\text{GGM}}.$$
 (14)

The criterion for the detection of outliers was considered as expected values that were all within the interval $[-2\sigma + 2\sigma]$. The 2- σ criterion was established empirically, considering a normal distribution for which the probability that a value ($N_{\rm GNSS/lev} - N_{\rm GGM}$) belongs to the set of expected values is at least 95.45%.

The statistics for ΔN , before and after outlier exclusion, are shown in Table 3.

High maximum/minimum and standard deviation values for ΔN statistics (before outlier exclusion) shown in Table 3 are due to gross errors in heights (leveled/ellipsoidal), registered in the observation, processing, or handling of data collection's stages.

Furthermore, Table 3 shows the extreme values close to 1 m and the standard deviation of 0.3791 m calculated after eliminating 104 records detected as outliers. These values are graphically represented in the frequency distribution of Figure 4, in which, additionally, it can be seen that approximately 61% of the calculated ΔN are in the range [-0.4 to 0.2] m.

Figure 5 shows the spatial distribution of the resulting discrepancies ($N_{\rm GNSS/lev}-N_{\rm XGM2019e}$). An increase in N_r values is observed in the Andes mountain range region, whose highest heights in Ecuador are located approximately between longitudes 79°W and 77°W (Figure 5). This is explained by the fact that in mountainous regions, the omission error of the GGM tends to increase due to deficiencies in the representation of the topographic masses effect for gravity field modeling (high frequency of the gravity field).

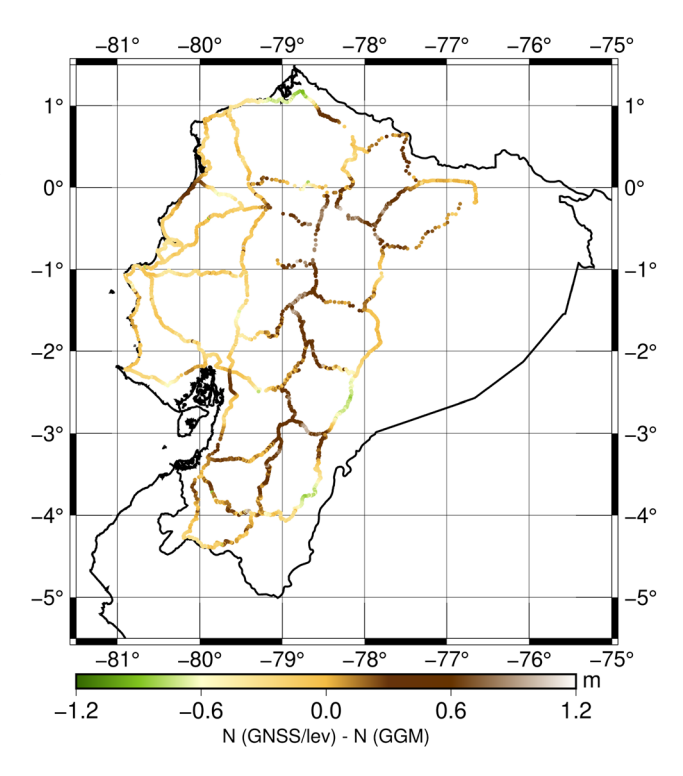


Figure 5: $N_{\text{GNSS/lev}} - N_{\text{GGM}}$.

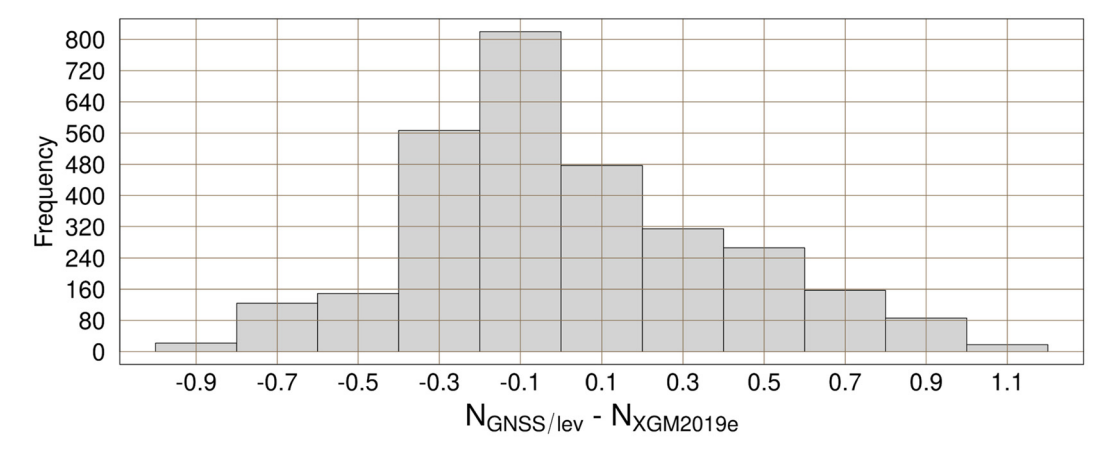


Figure 4: Frequency distribution for $N_{GNSS/lev} - N_{GGM}$ (m).

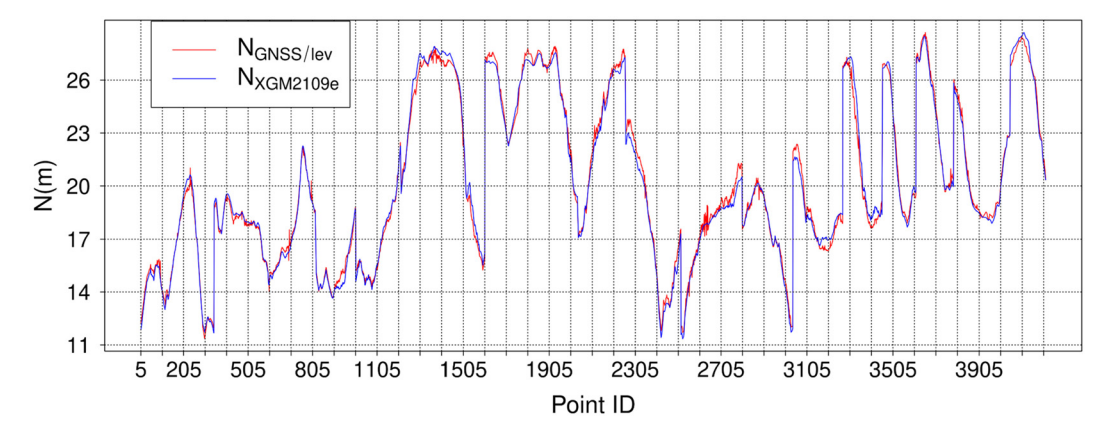


Figure 6: N_{GNSS/lev} and geoid heights from XGM2019e.

The calculated ΔN are interpreted through the degree of adherence of the two series observed in Figure 6, which shows the values of N and $N_{\rm XGM2019e}$ for all points considered in the analysis. Discrepancies between geoid heights from GNSS/lev records and those from the GGM XGM2019e are mainly due to errors that affect the accuracy of leveled and ellipsoidal heights, omission/commission errors of GGMs, inconsistencies in the local datum, and systematic effects.

Model omission errors tend to increase in mountainous regions due to deficiencies in the representation of the effect of topographic masses on the gravity field. Figure 7 shows the variation of geoid heights and ΔN ($N-N_{\rm XGM2019e}$) as a function of orthometric height (a) and longitude (b). The influence of the mountainous region's topographic masses (the Andes mountain range) can be interpreted in Figure 7(a), in which a slightly increasing tendency of geoid heights associated with the increase in orthometric heights can be observed. In Figure 7(b), it is observed that the computed and modeled N values and also the corresponding ΔN values, increasing in the rank of longitudes corresponding to the Andean region.

3 GGMs assessment based on geoid heights

Once outliers had been eliminated from the GNSS/lev dataset, the analysis oriented to the assessment of several combined GGMs was carried out. In this study, the combined GGMs shown in Table 1, considering their maximum degree, were evaluated. The analysis was performed in terms of geoid height discrepancies (ΔN) in equation (14), following for its calculation the same approach that was used for the outlier detection stage. The statistics for ΔN are shown in Table 4.

The standard deviation, in all cases, exceeds 40 cm, with the smallest value corresponding to the GGM XGM2019e. The expected accuracy of the GGM for the study region is in the range of [40, 47] cm, with mean values close to [20, 24] cm. As can be seen in the frequency distribution in Figure 8, for all cases, approximately 70% of ΔN are in the range [–50 50] cm, while the interquartile range, as shown in Figure 9, is approximately [–20 30] cm.

As an additional element, regarding the statistical analysis, correlations (Corr.) close to 1 between the calculated geoid heights and those derived from the GGMs (Table 4) are shown graphically in Figure 10.

Moreover, based on the approach proposed by Kotsakis and Sideris (1999) and following the analysis carried out by Tocho et al. (2022), the discrepancies between the calculated and modeled geoid heights are minimized by adjusting the parameters of the following formula:

$$N_{\text{GNSS/lev}} - N_{\text{GGM}} = a_i^T x + v_i, \tag{15}$$

where v_i are the residuals, and $a_i^T x$ can be calculated as follows (Kotsakis and Katsambalos, 2010):

$$a_i^T x = a + b \cos \varphi_i \cos \lambda_i + c \cos \varphi_i \sin \lambda_i + d \sin \varphi_i$$
, (16)

where φ_i and λ_i are the latitudes and longitudes for the GNSS/lev records, and a, b, c, and d are the parameters calculated by the least-squares method.

Thus, by the least-squares adjustment, a correction surface, established by the computed parameters (four-parameter model), was estimated for each GGM, minimizing the residuals (v_i) of equation (15) and theoretically minimizing local vertical datum inconsistencies and systematic errors of the datasets (Tocho et al., 2022). Analogous to the statistics presented in Table 4, new statistics were calculated this time considering the geoid heights affected by the correction surface.

8 — José Carrión et al. DE GRUYTER

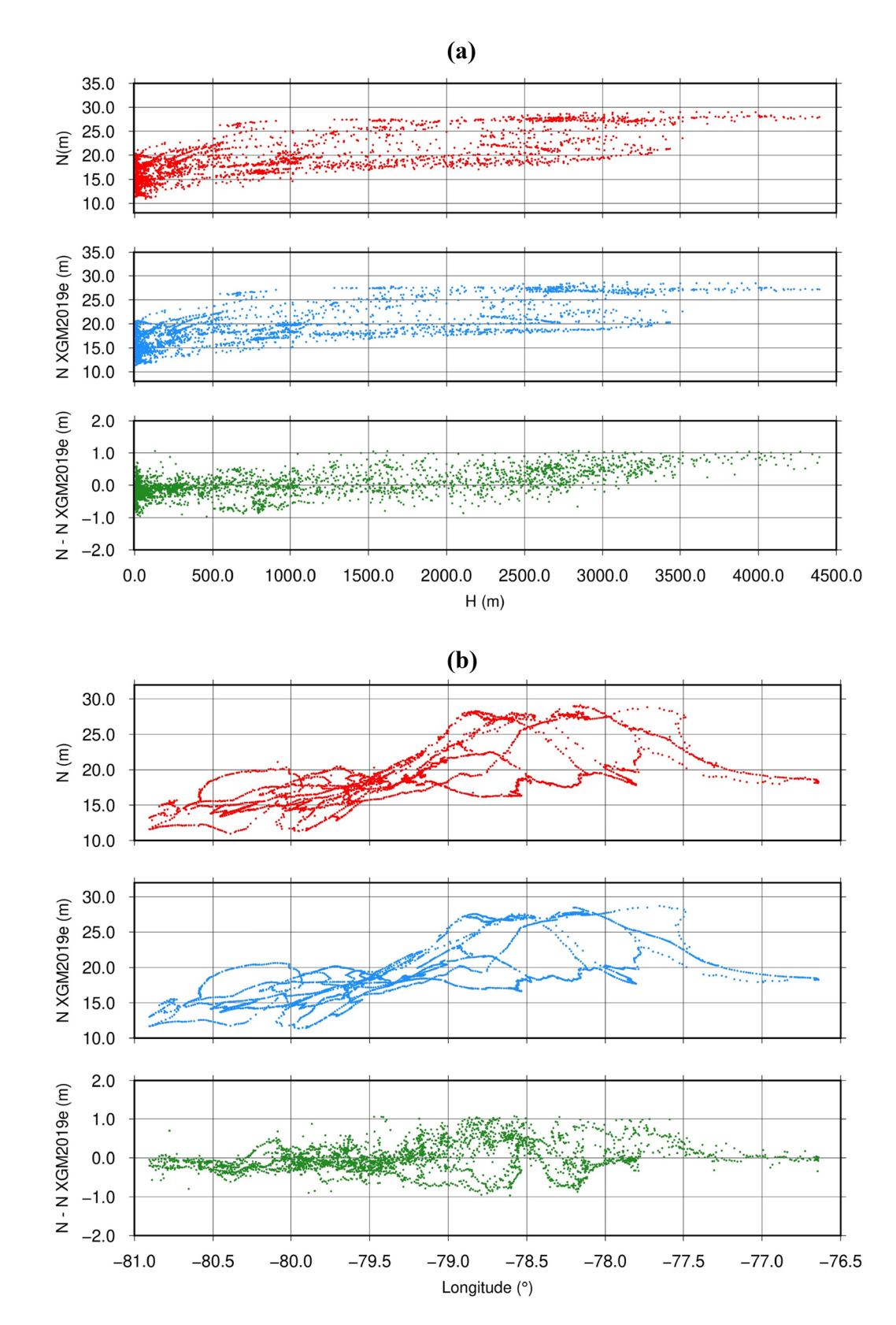


Figure 7: (a) $N_{\rm GNSS/lev}$, $N_{\rm XGM2019e}$, and $N_{\rm res}$ vs $H_{\rm ort}$. (b) $N_{\rm GNSS/lev}$, $N_{\rm XGM2019e}$, and $N_{\rm res}$ vs longitude.

Table 4: Geoid discrepancies (ΔN) statistics

GGM	Min. (m)	Max. (m)	Mean (m)	Std. (m)	Corr.
EIGEN6c4	-1.226	1.784	0.229	0.421	0.996
EGM2008	-1.652	1.989	0.239	0.469	0.995
GECO	-1.132	1.952	0.233	0.433	0.996
SGG-UGM-1	-1.310	1.800	0.215	0.420	0.996
SGG-UGM-2	-1.295	1.824	0.226	0.417	0.996
XGM2019e	-1.490	2.135	0.208	0.407	0.997

The statistics for ΔN (Table 5), after applying the correction surface, show for all the cases a reduction in the standard deviations (Std.), with a value of 0.355 m for XGM2019e, which best fits the geoid heights from the GNSS/lev records. Furthermore, for all cases, the null mean values denote the influence of an offset on the reference surface.

Figure 11 shows the standard deviations for the adjusted and unadjusted geoid height discrepancies (ΔN). For all cases,

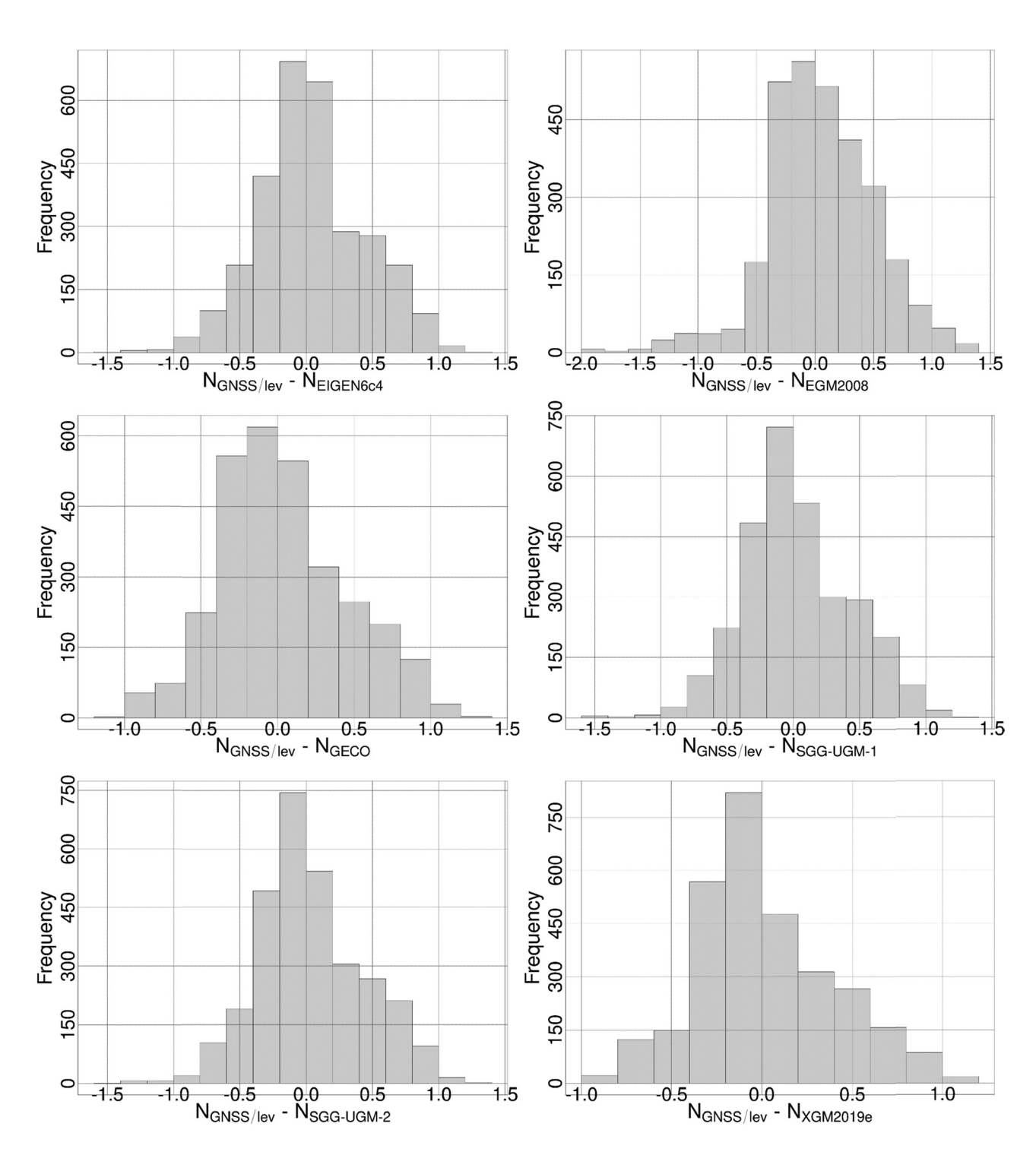


Figure 8: Frequency distribution for $N_{GNSS/lev} - N_{GGM}$.

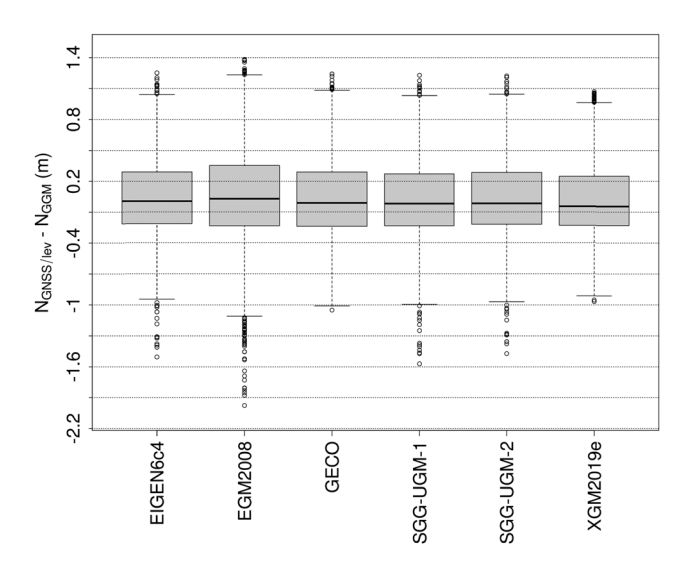


Figure 9: Boxplot for $N_{\text{GNSS/lev}} - N_{\text{GGM}}$.

there is a decrease in the Std. of about 5 cm. Note also that, according to the Std., the worst agreement between GNSS/lev and GGMs geoid heights corresponds to EGM2008, for which Std. of 0.469 and 0.440 m were calculated for the unadjusted and adjusted geoid heights, respectively.

According to Tocho et al. (2022), the previously described procedure generates a deformed surface (geoid) that better fits the GNSS/lev records, and only a pure gravimetric geoid can be used for the determination of IHRS coordinates. Therefore, this surface cannot be used to determine geopotential values in the context of the IHRS realization. However, the described procedure allows for estimating the effects related to datum inconsistency and other systematic effects contained in the data sets.

4 GGMs assessment based on geopotential values

As a second stage in the evaluation of the GGMs, the analysis was carried out in terms of geopotential values, which were compared with the corresponding value calculated for the EVD (*La Libertad* tide gauge) through the fixed solution of the GBVP (Carrión et al., 2023).

According to Barthelmes (2013), the geopotential is calculated as follows:

$$W(r, \lambda, \varphi) = \frac{GM}{r} \sum_{\ell=0}^{\ell} \sum_{m=0}^{\max} \sum_{m=0}^{\ell} \left(\frac{R}{r} \right)^{\ell} P_{\ell m} (\sin \varphi) (C_{\ell m}^{W} \cos m\lambda) + S_{\ell m}^{W} \sin m\lambda),$$
(17)

where r,λ , and φ are the spherical geocentric coordinates of the computation point; and $C_{\ell m}^W$ and $S_{\ell m}^W$ are the fully normalized spherical harmonic coefficients.

The geopotential value for the EVD (equation (17)) was obtained from the ICGEM calculation service, considering the maximum degree for the evaluated GGMs, the zero-tide as permanent tide concept, and finally the zero-degree term was included.

Because W_0 is determined using the conventions defined by the IAG, the zero-degree term must be considered in the context of the unification of vertical reference systems and the establishment of the IHRF. However, the calculation of quantities originating from GGM is independent of this term and should only be considered to rescale these quantities in relation to a given geoid (equipotential surface).

As recommended by Sánchez et al. (2021), the calculations were performed in the zero-tide concept, and later, the geopotential values were transformed into the meantide concept. According to Mäkinen (2017), this transformation is performed by including the latitude depending on the term W_T .

$$W_T = 0.9722 - 2.8841 \sin^2 \varphi - 0.0195 \sin^4 \varphi \, [\text{m}^2 \text{s}^{-2}].$$
 (18)

The differences between the calculated and the modelled values of the GGMs vary between approximately 0.01 and $1.25\,\mathrm{m^2\,s^{-2}}$, with the XGM2019e (as in the case of the analysis for geoid heights) being the model that best approximates the geopotential value calculated through the fixed GBVP solution. Eigen6c4, on the other hand, presents a considerably higher difference in relation to the other models. The corresponding differences in terms of geopotential values are shown in Table 6.

Figure 12 shows the differences found in this analysis graphically.

5 Conclusions

As a result of the GGM validation based on the comparison of geoid heights with GNSS/lev records in Ecuador, it was found that the expected accuracy of the GGM for the study region is in the range of [40, 47] cm and the mean values are in the range of [20, 24] cm.

The comparison of GGM geopotential values with the corresponding value obtained through the GBVP solution denotes that the differences between the calculated and the modelled values of the GGMs vary approximately between 0.01 and 1.25 $\rm m^2~s^{-2}$.

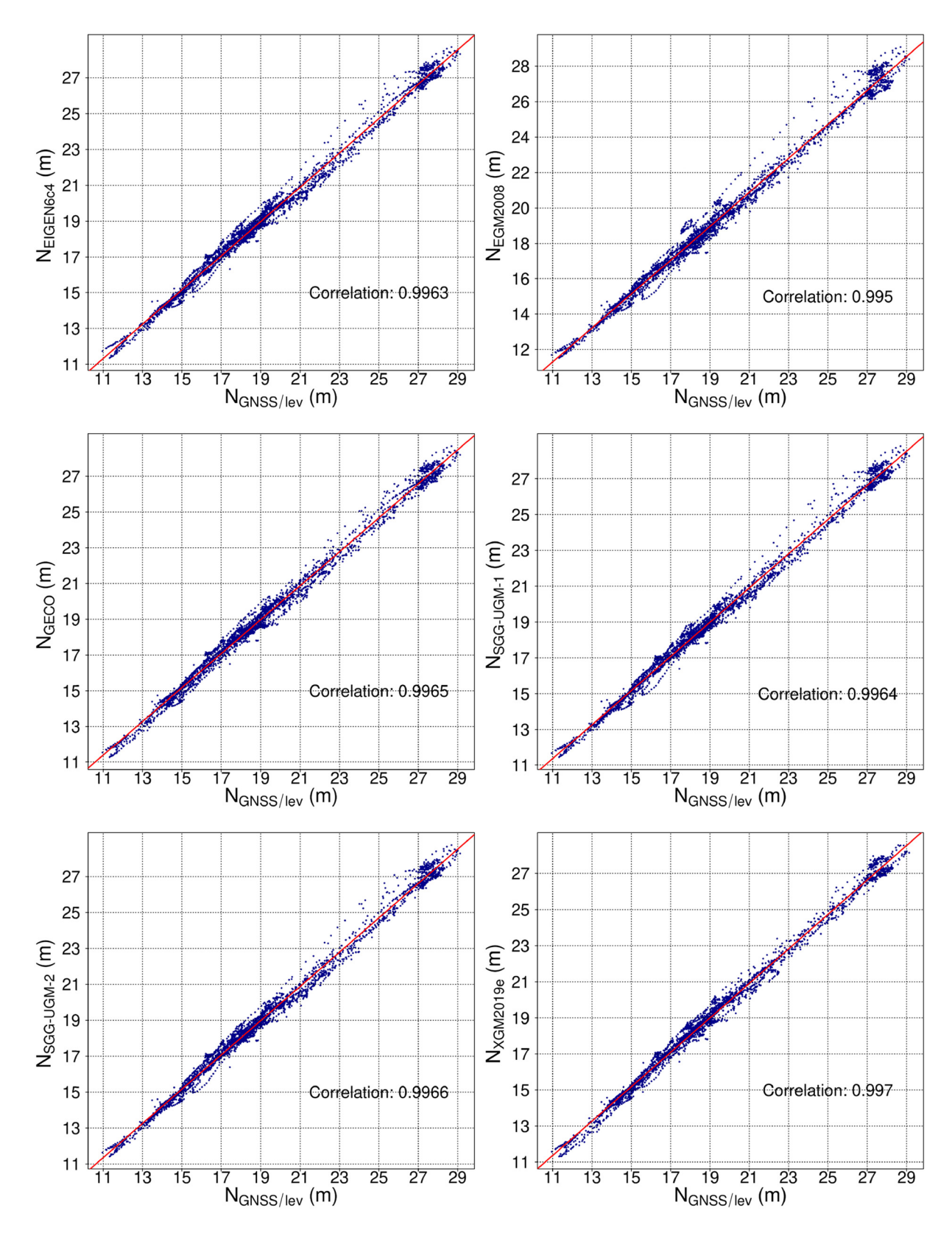


Figure 10: $N_{\rm GNSS/lev}$ and $N_{\rm GGM}$ correlation.

Table 5: Adjusted ΔN statistics

GGM	Min. (m)	Max. (m)	Mean (m)	Stdv. (m)	Corr.
EIGEN6c4	-1.784	1.165	0.000	0.373	0.996
EGM2008	-2.191	1.265	0.000	0.440	0.995
GECO	-1.323	1.088	0.000	0.380	0.996
SGG-UGM-1	-1.183	1.113	0.000	0.371	0.997
SGG-UGM-2	-1.758	1.104	0.000	0.363	0.997
XGM2019e	-1.095	1.095	0.000	0.355	0.997

For the two analyses carried out (with geoid heights and geopotential values), the model with the best performance was the XGM2019e.

Authors as Rummel (2012), Sánchez and Sideris (2017), have concluded that the expected mean accuracy for the GGMs in well-surveyed areas is ± 0.4 to ± 0.6 m² s⁻², and ± 2 to ± 4 m² s⁻² for sparsely surveyed areas. In this sense, in relation to the potential differences in Table 6 [$\sim 0.01 \sim 1.25$] m² s⁻², we can mention that, although the values obtained

Table 6: Height anomalies and potential values, calculated/modelled comparison

GGM	$W_{\rm GBVP} - W_{\rm GGM} (\rm m^2 s^{-2})$		
Eigen6C4	1.246		
EGM2008	0.339		
GECO	-0.313		
SGG-UGM-1	0.537		
SGG-UGM-2	0.671		
XGM2019e	0.012		

are close to the range that corresponds to well-surveyed areas, it is not possible to carry out an analysis in terms of precision because these values are estimated for a single point.

According to Ihde et al. (2017), although the target accuracy for the IHRS geopotential numbers is $0.01\,\mathrm{m}^2$ s⁻², in practice, this value is in a range of $0.1\text{--}1\,\mathrm{m}^2$ s⁻². This is due to factors such as non-unified standards for:

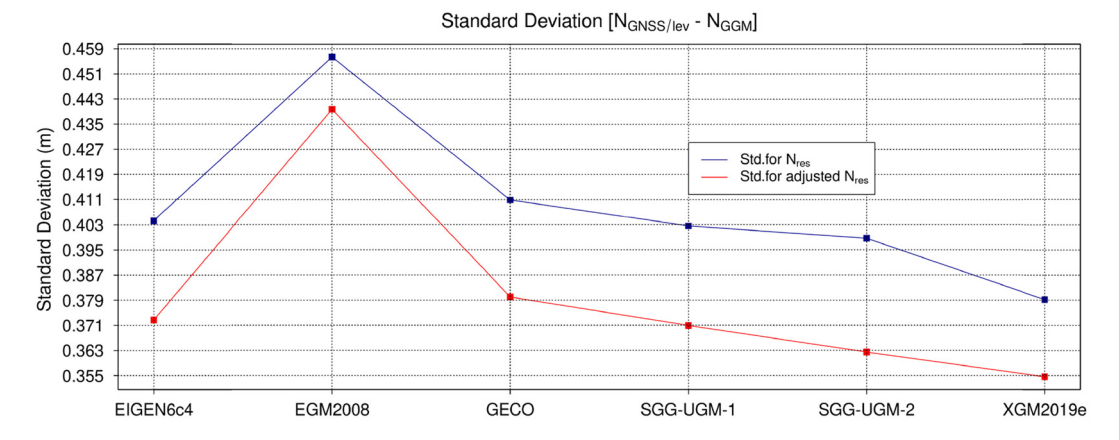


Figure 11: Std. $[N_{GNSS/lev} - N_{GGM}]$.

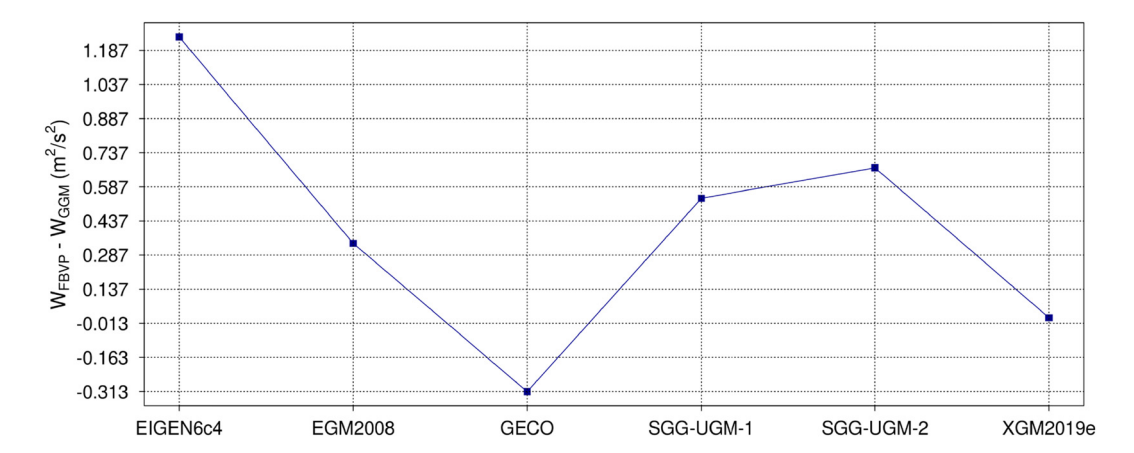


Figure 12: Calculated/modeled geopotential differences.

determination of potential values, gravitational field modeling, estimation of position vectors, heterogeneity in the distribution of references that make up the geodetic infrastructure, etc. Thus, the estimated accuracies for the GGM in Ecuador, which are at least 2 orders lower than the target value, allow us to conclude that the determination of geopotential values, exclusively from GGMs, for IHRF fundamental stations in Ecuador is not feasible.

The zero-degree term considered in the calculation of geoid heights has an approximate value of -17 cm. Its influence on the calculation is not negligible, and it was one of the main causes of discrepancies in the results obtained for the Colorado experiment, carried out for the standardization of geopotential calculation procedures in the context of the establishment of the IHRS (Wang et al., 2021).

To be consistent, and following the recommendations given by the IAG on the IHRS realization, the calculations were performed in the zero-tide concept, and at the end of the calculation procedure, the geopotential values were transformed to the mean-tide concept.

Orthometric heights were calculated with the aim of giving a physical meaning to heights used in the analyses carried out in this study.

Through an adjustment based on the least-squares criterion, a surface that best fits the geoid heights of the GNSS records/lev was established. However, the adjustment reduces the discrepancies between the GNSS/lev geoid heights and the GGM's values, and this procedure generates a deformed surface that cannot be used to determine geopotential values in the context of the IHRS realization.

Acknowledgements: The authors would like to express their gratitude to the Military Geographic Institute of Ecuador for the support and the GNSS/lev data. The authors also thank the editor and reviewers for their valuable contribution.

Conflict of interest: Authors state no conflict of interest.

References

- Altamimi, Z., P. Rebischung, L. Métivier, and X. Collilieux. 2016. "ITRF2014: A new release of the International Terrestrial Reference Frame modeling nonlinear station motions." Journal of Geophysical Research: Solid Earth 121(8), 6109-6131. doi: 10.1002/2016JB013098.
- Barthelmes, F. 2013. Definition of functionals of the geopotential and their calculation from spherical harmonic models: Theory and formulas used by the calculation service of the International Centre for Global Earth Models (ICGEM).
- Blitzkow, D., A. de Matos, and S. Costa, 2017. Primeros esfuerzos para el establecimiento del IHRF en Brasil. Simposio SIRGAS 2017.

- Carrión, J. L., S. R. C. De Freitas, and R. Barzaghi. 2023. "On the connection of the Ecuadorian Vertical Datum to the IHRS." Journal of Geodetic Science 13(1), 1-20. doi: 10.1515/jogs-2022-0151.
- Carrión Sánchez, J. L., S. R. C. de Freitas, and R. Barzaghi. 2018. "Offset evaluation of the Ecuadorian Vertical Datum related to the IHRS." Boletim de Ciencias Geodesicas 24(4), 503-524. doi: 10.1590/S1982-21702018000400031.
- Drewes, H. 1976. Berechnung regionaler Geoidundulationen durch gravimetrisches Nivellement mit Prädiktion der Schwereanomalien. Wissenschaftliche Arbeiten der Lehrstühle für Geodäsie, Photogrammetrie und Kartographie an der Technischen Universität Hannover.
- Drewes, H. 1978. "Experiences with least squares collocation as applied to interpolation of geodetic and geophysical quantities." XII Symposium on Mathematical Geophysics.
- Drewes, H., F. Kuglitsch, J. Adám, and R. Szabolcs. 2016. "The geodesist's Handbook 2016." Journal of Geodesy 90(10), 907-1205. doi: 10.1007/ s00190-016-0948-z.
- Drinkwater, M. R., R. Floberghagen, R. Haagmans, D. Muzi, and A. Popescu. 2003. "GOCE: ESA's first Earth Explorer Core mission." vol. 18, p. 419-432. Noordwijk, The Netherlands: European Space Agency. doi: 10.1007/978-94-017-1333-7_36.
- Ekman, M. 1989. "Impacts of geodynamic phenomena." Bulletin Géodésique 63(1), 281-296.
- Förste, C., S. Bruinsma, O. Abrikosov, F. Flechtner, J.-C. Marty, J.-M. Lemoine, C. Dahle, H. Neumayer, F. Barthelmes, R. König, R. Biancale, C. Förste, S. Bruinsma, O. Abrikosov, F. Flechtner, and J. Marty. 2014. "EIGEN-6C4 - The latest combined global gravity field model including GOCE data up to degree and order 1949 of GFZ Potsdam and GRGS Toulouse." EGU General Assembly 16, 3707. doi: 10.5880/icgem.2015.1.
- Gilardoni, M., M. Reguzzoni, and D. Sampietro. 2016. "GECO: A global gravity model by locally combining GOCE data and EGM2008." Studia Geophysica et Geodaetica 60(2), 228-247. doi: 10.1007/s11200-015-1114-4.
- Guimarães, G., D. Blitzkow, A. de Matos, V. Silva, and M. Inoue. 2022. "O estabelecimento do IHRF no Brasil: Situação atual e perspectivas futuras." Revista Brasileira de Cartografía 74(3), 651-670. doi: 10. 14393/rbcv74n3-64949.
- Guimarães, G., A. de Matos, A. Pereira, E. Antokoletz, I. Carrión, and L. Sánchez, 2021. "An overview of SIRGAS activities towards the IHRF." Scientific Assembly of the International Association of Geodesy.
- Heikkinen, M. 1978. On the tide-generating forces (Vol. 85). Helsinki: Publications of the Finnish Geodetic Institute, 85, 1978. https:// books.google.com.br/books?id=5ZYQAQAAMAAJ.
- Heiskanen, W. A. and H. Moritz. 1985. Geodesia Física. Madrid, Spain: Instituto Geográfico Nacional, Ed.
- Heiskanen, W. A. and H. Moritz. 1967. "Physical geodesy." Bulletin Géodésique (1946-1975) 86(1), 491-492.
- Hofmann-Wellenhof, B., and H. Moritz. 2006. Physical geodesy. Graz, Austria: Springer Science & Business Media.
- Ihde, J., L. Sánchez, R. Barzaghi, H. Drewes, C. Foerste, T. Gruber, G. Liebsch, U. Marti, R. Pail, and M. Sideris. 2017. "Definition and proposed realization of the International Height Reference System (IHRS)." Surv Geophys 38, 549-570. doi: 10.1007/s10712-017-9409-3.
- Ince, E., F. Barthelmes, S. Reißland, K. Elger, C. Förste, F. Flechtner, and H. Schuh. 2019. "ICGEM-15 years of successful collection and distribution of global gravitational models, associated services, and future plans." Earth System Science Data 11(2), 647-674. doi: 10.5194/ essd-11-647-2019.

- Kotsakis, C. and K. Katsambalos. 2010. "Quality analysis of global geopotential models at 1542 GPS/levelling benchmarks over the Hellenic mainland." *Survey Review* 42(318), 327–344. doi: 10.1179/003962610X12747001420500.
- Kotsakis, C., and M. G. Sideris. 1999. "On the adjustment of combined GPS/levelling/geoid networks." *Journal of Geodesy* 73(8), 412–421. doi: 10.1007/s001900050261.
- Lemoine, F. G., D. E. Smith, L. Kunz, R. Smith, E. C. Pavlis, N. K. Pavlis, S. M. Klosko, D. S. Chinn, M. H. Torrence, R. G. Williamson, C. M. Cox, K. E. Rachlin, Y. M. Wang, S. C. Kenyon, R. Salman, R. Trimmer, R. H. Rapp, and R. S. Nerem. 1997. "The development of the NASA GSFC and NIMA joint geopotential model." In: *Gravity, Geoid and Marine Geodesy* July, p. 461–469. Tokyo, Japan: International Association of Geodesy. doi: 10.1007/978-3-662-03482-8_62.
- Liang, W. and S. Reißland. 2018. SGG-UGM-1: the high resolution gravity field model based on the EGM2008 derived gravity anomalies and the SGG and SST data of GOCE satellite. GFZ Data Services. doi: 10.5880/icgem.2018.001.
- Liang, W., J. Li, X. Xu, S. Zhang, and Y. Zhao. 2020. "A high-resolution Earth's gravity field model SGG-UGM-2 from GOCE, GRACE, satellite altimetry, and EGM2008." *Engineering* 6(8), 860–878. doi: 10.1016/j. eng.2020.05.008.
- Mäkinen, J. 2017. *The permanent tide and the International Height Reference System IHRS*. IAG-IASPEI Joint Scientific Assembly.
- Meissl, P. 1981. *The use of finite elements in physical geodesy. Geodetic Science and Surveying*, *313*. The Ohio State University. https://apps.dtic.mil/sti/pdfs/ADA104164.pdf.
- Pavlis, N. K. 2013. "Global gravitational models." In: *Geoid determination: Theory and methods*, edited by Sansò, F. and M. G. Sideris, p. 261–310. Berlin, Heidelberg: Springer. doi: 10.1007/978-3-540-74700-0_6.
- Pavlis, N. K, S. A. Holmes, S. C. Kenyon, and J. K. Factor. 2012. "The development and evaluation of the Earth Gravitational Model 2008 (EGM2008)." *Journal of Geophysical Research: Solid Earth* 117(B4), 1–38. doi: 10.1029/2011|B008916.
- Pavlis, N. K., S. A. Holmes, S. C. Kenyon, and J. K. Factor. 2008. "An earth gravitational model to degree 2160: EGM2008." Presented at the 2008 General Assembly of the European Geosciences Union, Vienna, Austria, April 13–18, Vol. 84, No. 1, pp. 2–4. http://earth-info.nga.mil/GandG/wqs84/gravitymod/egm2008/README_WGS84_2.pdf.
- Rapp, R. 1997. "Use of potential coefficient models for geoid undulation determinations using a spherical harmonic representation of the height anomaly/geoid undulation difference." *Journal of Geodesy* 71(5), 282–289. doi: 10.1007/s001900050096.
- Rapp, R. 1989. "The treatment of permanent tidal effects in the analysis of satellite altimetry data for sea surface topography." *Manuscripta Geodaetica* 14, 368–372.
- Rummel, R. 2012. "Height unification using GOCE." *Journal of Geodetic Science* 2(4), 355–362. doi: 10.2478/v10156-011-0047-2.

- Rummel, R., G. Balmino, J. Johannessen, P. Visser, and P. Woodworth. 2002. "Dedicated gravity field missions Principles and aims." *Journal of Geodynamics* 33(1–2), 3–20. doi: 10.1016/S0264-3707(01) 00050-3.
- Sánchez, L., J. Ågren, J. Huang, Y. M. Wang, J. Mäkinen, R. Pail, R. Barzaghi, G. S. Vergos, K. Ahlgren, and Q. Liu. 2021. "Strategy for the realisation of the International Height Reference System (IHRS)." Journal of Geodesy 95(3), 1–33. doi: 10.1007/s00190-021-01481-0.
- Sánchez, L., and M. G. Sideris. 2017. "Vertical datum unification for the International Height Reference System (IHRS)." *Geophysical Journal International* 209(2), 570–586. doi: 10.1093/qji/qqx025.
- SIRGAS WG-III. 2021. Guía para la selección de estaciones IHRF. https://sirgas.ipgh.org/docs/Guias/Guia%20para%20la%20seleccion%20de %20estaciones%20IHRF.pdf.
- Sünkel, H. 1981. Point mass models and the anomalous gravitational field. Report No. 328. The Ohio State University, Dept. of Geodetic Science, Columbus, Ohio, 40 p. https://apps.dtic.mil/sti/tr/pdf/ADA115216.pdf
- Sünkel, H. 1984. Splines: their equivalence to collocation. Report No. 357. The Ohio State University, Dept. of Geodetic Sciences, Columbus, Ohio, 55 p.
- Tapley, B. D., S. Bettadpur, M. Watkins, and C. Reigber. 2004. "The gravity recovery and climate experiment: Mission overview and early results." *Geophysical Research Letters* 31(9), 1–4. doi: 10.1029/2004GL019920.
- Tocho, C. and G. S. Vergos. 2016. "Estimation of the geopotential value W₀ for the local vertical datum of Argentina using EGM2008 and GPS/levelling data W₀^{LVD}." In C. Rizos and P. Willis (Eds.), *IAG 150 Years: Proceedings of the IAG Scientific Assembly in Postdam, Germany, 2013* (pp. 271–279). Springer International Publishing. doi: 10.1007/1345_2015_32.
- Tocho, C. N., E. D. Antokoletz, A. R. Gómez, H. Guagni, and D. A. Piñon. 2022. "Analysis of high-resolution global gravity field models for the estimation of International Height Reference System (IHRS) coordinates in Argentina." *Journal of Geodetic Science* 12(1), 131–140. doi: 10.1515/jogs-2022-0139.
- Tocho, C. N., E. D. Antokoletz, and D. A. Piñón. 2023. "Towards the realization of the International Height Reference Frame (IHRF) in Argentina." *International Association of Geodesy Symposia*, 152, 11–20. doi: 10.1007/1345_2020_93.
- Torge, W. and J. Müller. 2012. "Geodesy." *De Gruyter Textbook*. Berlin, Germany: De Gruyter.
- Wang, Y. M., L. Sánchez, J. Ågren, J. Huang, R. Forsberg, H. A. Abd-Elmotaal, K. Ahlgren, R. Barzaghi, T. Bašić, D. Carrion, S. Claessens, B. Erol, S. Erol, M. Filmer, V. N. Grigoriadis, M. S. Isik, T. Jiang, Ö. Koç, J. Krcmaric, ... P. Zingerle. 2021. "Colorado geoid computation experiment: overview and summary." *Journal of Geodesy* 95(12), 127. doi: 10.1007/s00190-021-01567-9.
- Zingerle, P., R. Pail, T. Gruber, and X. Oikonomidou. 2020. "The combined global gravity field model XGM2019e." *Journal of Geodesy* 94(7), 1–12. doi: 10.1007/s00190-020-01398-0.